Original Article | Pediatric Imaging

https://doi.org/10.3348/kjr.2018.19.1.111
pISSN 1229-6929 · eISSN 2005-8330
Korean J Radiol 2018;19(1):111-118

Korean Journal of Radiology
KJR

Four-Dimensional CT of the Diaphragm in Children: Initial Experience

Hyun Woo Goo, MD, PhD

Department of Radiology and Research Institute of Radiology, University of Ulsan College of Medicine, Asan Medical Center, Seoul 05505, Korea

Objective: To evaluate the technical feasibility of four-dimensional (4D) CT for the functional evaluation of the pediatric diaphragm.

Materials and Methods: In 22 consecutive children (median age 3.5 months, age range 3 days–3 years), 4D CT was performed to assess diaphragm motion. Diaphragm abnormalities were qualitatively evaluated and diaphragm motion was quantitatively measured on 4D CT. Lung density changes between peak inspiration and expiration were measured in the basal lung parenchyma. The diaphragm motions and lung density changes measured on 4D CT were compared between various diaphragm conditions. In 11 of the 22 children, chest sonography was available for comparison.

Results: Four-dimensional CT demonstrated normal diaphragm (n = 8), paralysis (n = 10), eventration (n = 3), and diffusely decreased motion (n = 1). Chest sonography demonstrated normal diaphragm (n = 2), paralysis (n = 6), eventration (n = 2), and right pleural effusion (n = 1). The sonographic findings were concordant with the 4D CT findings in 90.9% (10/11) of the patients. In diaphragm paralysis, the affected diaphragm motion was significantly decreased compared with the contralateral normal diaphragm motion (-1.1 ± 2.2 mm vs. 7.6 ± 3.8 mm, p = 0.005). The normal diaphragms showed significantly greater motion than the paralyzed diaphragms (4.5 ± 2.1 mm vs. -1.1 ± 2.2 mm, p < 0.0001), while the normal diaphragm motion was significantly smaller than the motion of the contralateral normal diaphragm in paralysis (4.5 ± 2.1 mm vs. 7.6 ± 3.8 mm, p = 0.01). Basal lung density change of the affected side was significantly smaller than that of the contralateral side in diaphragm paralysis (89 ± 73 Hounsfield units [HU] vs. 180 ± 71 HU, p = 0.03), while no significant differences were found between the normal diaphragms and the paralyzed diaphragms (136 ± 66 HU vs. 89 ± 73 HU, p = 0.1) or between the normal diaphragms and the contralateral normal diaphragms in paralysis (136 ± 66 HU vs. 180 ± 71 HU, p = 0.1).

Conclusion: The functional evaluation of the pediatric diaphragm is feasible with 4D CT in select children.

Keywords: *4D CT; Diaphragm; Child; Functional CT evaluation; Diaphragm paralysis; Diaphragm eventration; Chest sonography*

INTRODUCTION

The diaphragm, the primary muscle of ventilation, is commonly affected by phrenic nerve injury during cardiac surgery in both adults and children up to 25% and 75%, respectively (1-4). In symptomatic patients, surgical diaphragm plication and phrenic nerve stimulation may be considered as treatment options (1). On the contrary, a recovery from diaphragm dysfunction may be anticipated because the dysfunction is often transient in asymptomatic patients. However, it should be emphasized that children

Received May 26, 2017; accepted after revision July 25, 2017.
Corresponding author: Hyun Woo Goo, MD, PhD, Department of Radiology and Research Institute of Radiology, University of Ulsan College of Medicine, Asan Medical Center, 88 Olympic-ro 43-gil, Songpa-gu, Seoul 05505, Korea.
• Tel: (822) 3010-4388 • Fax: (822) 476-0090
• E-mail: ghw68@hanmail.net

are less tolerable to diaphragm dysfunction because the accessory muscles of respiration are not strong enough to compensate for the diaphragm dysfunction. Therefore, the prompt and accurate imaging diagnosis of diaphragm dysfunction is very important in children (3).

For the dynamic evaluation of diaphragm motion, fluoroscopy, sonography, and MRI may be used (1-3, 5). Of them, sonography is the imaging modality of choice and a suitable bedside procedure. However, sonography is limited by operator dependency and the non-assessable left diaphragm being obscured by bowel gas (4, 6). MRI may provide objective and accurate diagnosis of diaphragm dysfunction, but its wide use is restricted by limited availability, difficult scheduling, difficult patient preparation, and high costs. On the other hand, modern CT scanners with wide longitudinal coverages ranging from 4 to 16 cm can offer four-dimensional (4D) data acquisition, and have been used for the dynamic evaluation of the pediatric thorax (5, 7-10). However, it appears that 4D CT has not been used for the dynamic evaluation of the pediatric diaphragm. Therefore, the purpose of this study was to evaluate the technical feasibility and clinical usefulness of 4D CT for the functional evaluation of the pediatric diaphragm.

MATERIALS AND METHODS

Study Population

This retrospective study was approved by the local Institutional Review Board and all CT examinations were clinically requested. In all cases, 4D CT of the diaphragm was performed immediately after main chest or cardiac CT. Between July 2011 and September 2016, 22 consecutive children (median age 3.5 months, age range 3 days–3 years; M:F = 12:10) who underwent 4D CT to assess diaphragm motion, were included in this study. Underlying diseases of the study population included congenial heart disease (n = 17), repaired congenial diaphragmatic hernia (n = 2; right 1, left 1), developmental lung lesion (n = 2), and diaphragmatic eventration (n = 1; left). In four patients, diaphragm plication (right:left = 1:3) was performed prior to 4D CT examination. In 11 of the 22 children, chest sonography was available for comparison. At our institution, fluoroscopy is not used for evaluating diaphragm motion abnormality.

4D CT of the Diaphragm

Free-breathing 4D CT of the diaphragm was performed by using a 128-slice dual-source scanner (SOMATOM Definition Flash; Siemens Healthcare, Forchheim, Germany) with 2 x 64 x 0.6 mm slices with z-flying focal spot technique, a 0.75-mm slice width, and a 0.4-mm reconstruction interval. For 4D CT, a six-phase sequential scan with a longitudinal coverage of 3.8-cm and a temporal resolution of 210 msec was acquired without table movement for 2 seconds. As a result, a total of 570 axial images (95 images/phase x 6 phases) were generated for each patient. The scan position of 4D CT was adjusted on the scout image to include both diaphragms. To avoid image degradation caused by high image noise at low kV on non-contrast low-dose 4D CT images, 100 kV was used in all patients. To maintain diagnostic quality with minimal radiation exposure, a volume CT dose index value based on a 32-cm phantom was individually determined, based on the cross-sectional area and mean body density measured on an axial CT image obtained approximately 1–2 cm above the dome of the liver (11). However, radiation dose could not decrease beyond the limit (1.2 mGy) of volume CT dose index at 100 kV in 77.3% (17/22) of the patients. The volume CT dose index and dose-length product values (mean ± standard deviation) based on a 32-cm phantom of 4D CT were 1.3 ± 0.1 mGy and 5.1 ± 0.3 mGy·cm, respectively. Dose-length product-based effective dose values of 4D CT were not calculated because the conversion factors specific for the diaphragmatic region are unavailable. To sedate the patients, oral choral hydrate (50 mg/kg) was initially used and intravenous midazolam (0.1 mg/kg) or ketamine (1 mg/kg) was additionally administered as required.

Thin axial CT images were transferred to a multimodality workstation (Leonardo; Siemens Healthcare), and multiplanar 4D CT images of the diaphragm using thin-slab averaging or minimum intensity projection technique were reconstructed using software (Inspace; Siemens Healthcare). Quality of 4D CT images was evaluated by a pediatric radiologist with 17-years' experience of pediatric CT imaging.

Diaphragm abnormality was qualitatively evaluated and diaphragm motion was quantitatively measured on coronal reformatted 4D CT. Normal diaphragm motion was defined as normally expected downward motion during inspiration and normally expected upward motion during expiration. Diaphragm palsy was defined as mildly reduced motion, and diaphragm paralysis was defined as markedly

Korean Journal of Radiology
KJR

reduced motion, almost no motion, or paradoxical motion throughout the respiratory cycle. Diaphragm eventration was defined as a focal bulge of the diaphragm due to congenital thinning.

On our picture archiving and communication system (Petavision; Hyundai information technology, Seoul, Korea), the magnitude of diaphragm motion was measured at the middle portion of the diaphragm between the highest and the lowest positions throughout the respiratory cycle on coronal reformatted 4D CT by using calipers while scrolling the images in cine loop mode.

The qualitative and quantitative evaluations of 4D CT were conducted by a pediatric radiologist with 17 years of experience in pediatric CT imaging. Based on the qualitative and quantitative evaluation as described above, the diaphragms were categorized into normal diaphragm in normal patients, ipsilateral affected diaphragm and contralateral normal diaphragm in patients with unilateral diaphragm abnormalities, and affected diaphragm in patients with bilateral diaphragm abnormalities.

Since the degree of lung inflation and deflation throughout the respiration cycle may affect the degree of diaphragm motion, a lung density change in Hounsfield units (HU) between peak inspiration and peak expiration was measured by placing a rectangular region of interest (12.5 ± 3.9 mm^2) in the basal lung parenchyma while carefully avoiding the lung vessels and airways. In one patient, right basal lung density could not be measured due to extensive atelectasis.

Chest Sonography

B- and/or M-modes sonography was performed to evaluate diaphragm abnormality in 11 patients by using an ATL HDI 5000 scanner (Philips Healthcare, Best, the Netherlands) with a 5–8 MHz convex transducer by pediatric radiologists (less than 2 years of experience of chest sonography for evaluating diaphragm motion). In 3 of the 11 patients, only the morphologic evaluation was performed without diaphragm motion evaluation. The patients underwent chest sonography during spontaneous breathing, and patients with mechanically assisted ventilation, therefore, had the ventilator temporarily disconnected during chest sonography while being monitored by a physician. In addition to the morphologic evaluation of the diaphragm and adjacent organs, the diaphragm motion was assessed as previously described (4). However, the respiratory excursion of the diaphragm using M-mode was not measured. The inter-study interval between 4D CT and chest sonography was 7.7 ± 10.8 days (median 3 days, range 1–35 days). No operation was performed between 4D CT and chest sonography.

Statistical Analysis

Continuous variables are presented as mean ± standard deviation, or median with range, and categorical variables are expressed as frequency with percentage. Diaphragm motion and lung density change measured on 4D CT were compared between the right and left diaphragms with normal motion, and between the affected and contralateral normal diaphragms with abnormal motion for each patient using the Wilcoxon signed rank test. Moreover, diaphragm motion and lung density change measured on 4D CT were compared between the normal and abnormal diaphragms, and between the normal and contralateral normal diaphragms in different patients by utilizing the Mann-Whitney U test. A p value of less than 0.05 was considered to be statistically significant. Statistical analyses were performed using SPSS statistical software version 23.0 (IBM Corp., Armonk, NY, USA).

RESULTS

In all 22 patients, 4D CT examinations were successfully performed with diagnostic quality and no complications.

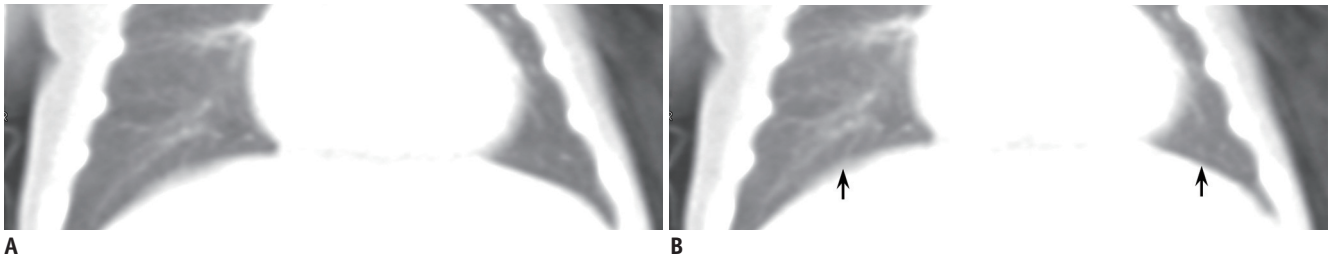

A **B**

Fig. 1. 3-day-old female newborn with congenital pulmonary airway malformation.
Coronal reformatted 4D CT images using thin-slab averaging technique obtained at peak inspiration **(A)** and peak expiration **(B)** demonstrate synchronous motion (arrows) of both diaphragms (right, 1.6 mm; left 1.8 mm). 4D = four-dimensional

4D CT of the Diaphragm vs. Chest Sonography

Four-dimensional CT demonstrated normal diaphragms in eight patients (Figs. 1, 2, Supplementary Movie 1 in the online-only Data Supplement), diaphragm paralysis in 10 (right:left = 6:4) (Fig. 3), diaphragm eventration in three (right:left = 1:2) (Fig. 4), and almost no motion diffusely involving both diaphragms in one. In the 8 patients showing normal diaphragm motion, additional 4D

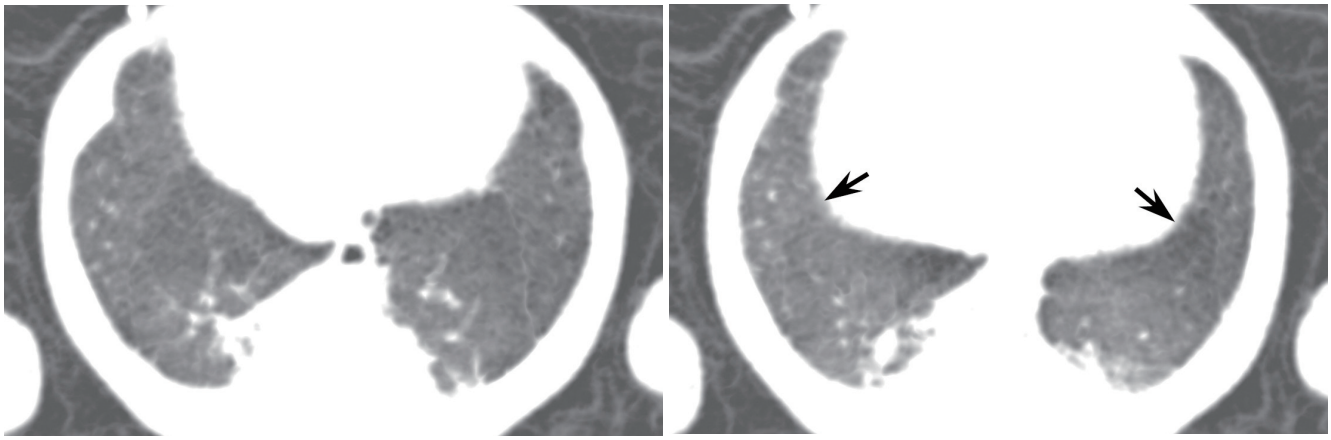

Fig. 2. 4-month-old male infant with chronic lung disease.
Oblique axial reformatted 4D CT minimum intensity projection images obtained at peak inspiration **(A)** and peak expiration **(B)** show simultaneous respiratory excursion (arrows) of both diaphragms (right, 4.8 mm; left 3.3 mm). Lung parenchymal lesions related to chronic lung disease are noted in posteromedial portions of both basal lungs.

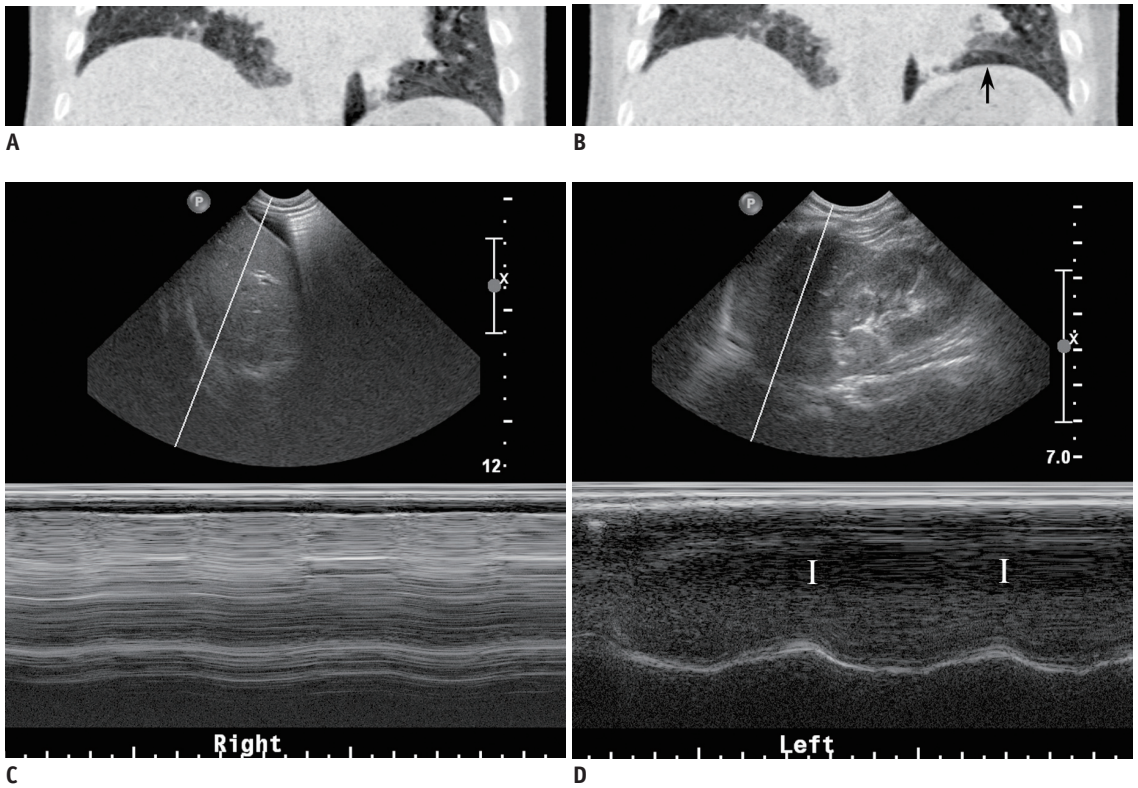

Fig. 3. 7-month-old male infant with double-outlet right ventricle, ventricular septal defect, and interrupted aortic arch who underwent aortic arch repair followed by pulsatile, bidirectional, cavopulmonary connection.
Coronal reformatted 4D CT minimum intensity projection images obtained at peak inspiration **(A)** and peak expiration **(B)** reveal almost no change in position of right diaphragm (1.8 mm) indicating right diaphragm paralysis. Left diaphragm shows normal motion (10.8 mm, arrow). **C**. M-mode sonography also shows almost no motion of right diaphragm as in 4D CT. **D**. M-mode sonography displays normal motion of left diaphragm with inspiration peaks (I).

Korean Journal of Radiology
KJR

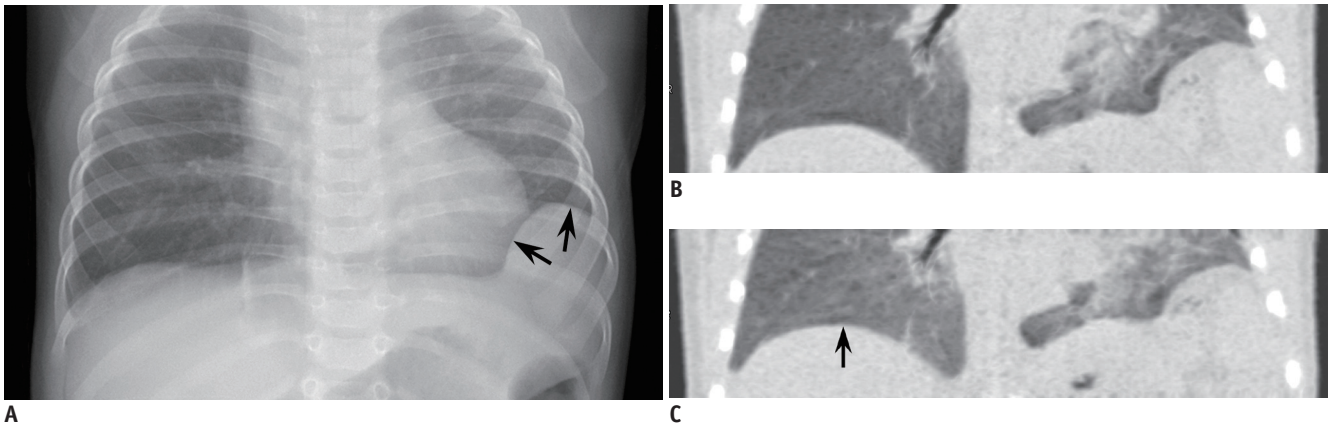

Fig. 4. 6-month-old female infant with left diaphragmatic eventration.
(A) Anteroposterior chest radiography shows focal bulge (arrows) at lateral portion of left diaphragm suggesting diaphragm eventration. Subsegmental atelectasis is noted in right basal lung. Coronal reformatted 4D CT minimum intensity projection images obtained at peak inspiration **(B)** and peak expiration **(C)** demonstrate markedly reduced motion of affected portion of left diaphragm (0.8 mm) as well as preserved motion of medial portion of left diaphragm (4.7 mm). Respiratory excursion (arrow) of normal right diaphragm was measured as 5.1 mm.

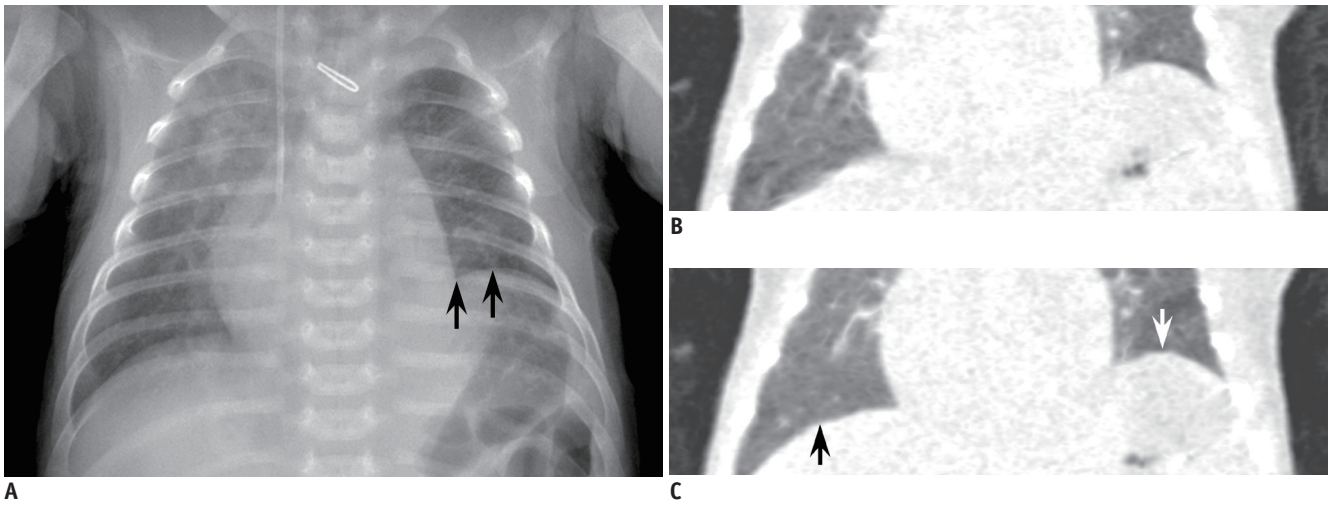

Fig. 5. 24-day-old male newborn who underwent aortic arch repair for interrupted aortic arch.
(A) Anteroposterior chest radiography reveals elevated left diaphragm (arrows) due to phrenic nerve injury during cardiac surgery. Increased opacities probably due to atelectasis in both lung fields, right central venous catheter, and surgical clip at aortic arch repair site are noted. Coronal reformatted 4D CT minimum intensity projection images obtained at peak inspiration **(B)** and peak expiration **(C)** demonstrate normal motion (black arrow) of right diaphragm (4.7 mm) and paradoxical motion (white arrow) of paralyzed left diaphragm (-5.1 mm).

CT was requested for the following indications: elevated left diaphragm, 3; suspected congenial diaphragmatic hernia, 2; status post left diaphragm plication, 1; status post repair of left diaphragmatic hernia, 1; and suspected diaphragm motion abnormality as a cause of respiratory difficulty, 1. In 6 of the 10 patients with diaphragm paralysis, paradoxical motion was observed in the affected diaphragm on 4D CT (Fig. 5, Supplementary Movie 2 in the online-only Data Supplement). In the 4 patients who underwent diaphragm plication, 4D CT showed normal diaphragms in one patient and diaphragm paralysis in three. In the 2 patients who underwent diaphragmatic hernia repair, 4D CT revealed normal diaphragms in one and diaphragm paralysis in one.

Chest sonography demonstrated normal diaphragms in 2 patients (no motion analysis in one), diaphragm paralysis in 6 (right:left = 4:2) (Fig. 3), diaphragm eventration in 2 (right:left = 1:1; no motion analysis in one), and right pleural effusion in 1 (no motion analysis). In contrast to 4D CT, paradoxical motion was detected by chest sonography in only 1 of the 6 patients with diaphragm paralysis. The sonographic findings were concordant with the 4D CT findings in 90.9% (10/11) of the patients except the 1 patient with right diaphragm paralysis and right pleural effusion. In this patient, chest sonography only detected right pleural effusion, and right diaphragm motion was not evaluated.

Table 1. Respiratory Excursions of Diaphragm Measured by 4D CT in Various Diaphragm Conditions

Diaphragm Conditions	Diaphragm Motion (mm)
Normal diaphragm (n = 16)	4.5 ± 2.1
Affected diaphragm in diaphragm paralysis (n = 10)	-1.1 ± 2.2
Contralateral normal diaphragm in diaphragm paralysis (n = 10)	7.6 ± 3.8
Affected diaphragm in diaphragm eventration (n = 3)	1.3 ± 1.1
Contralateral normal diaphragm in diaphragm eventration (n = 3)	4.1 ± 2.0
Ipsilateral normal diaphragm in diaphragm eventration (n = 2)*	4.5 ± 0.4
Affected diaphragm with bilaterally decreased motion (n = 2)	0.7 ± 0.3

*Respiratory excursion could not be measured in one patient with extensive diaphragm eventration. 4D = four-dimensional

Table 2. Basal Lung Density Change between Peak Inspiration and Peak Expiration Measured by 4D CT in Various Diaphragm Conditions

Diaphragm Conditions	Lung Density Change (HU)
Normal diaphragm (n = 16)	136 ± 66
Affected diaphragm in diaphragm paralysis (n = 9)*	89 ± 73
Contralateral normal diaphragm in diaphragm paralysis (n = 10)	180 ± 71
Affected diaphragm in diaphragm eventration (n = 3)	121 ± 83
Contralateral normal diaphragm in diaphragm eventration (n = 3)	183 ± 82
Affected diaphragm with bilaterally decreased motion (n = 2)	28 ± 19

*Right basal lung density could not be measured due to extensive atelectasis in one patient with right diaphragm paralysis. HU = Hounsfield units

Diaphragm Motion on 4D CT

The respiratory excursions of the diaphragm measured by 4D CT in various conditions are summarized in Table 1. In the 8 patients with normal diaphragms, no significant differences in the measured motion on 4D CT were found between the right and left diaphragms (4.9 ± 2.3 mm vs. 4.1 ± 1.9 mm, $p = 0.3$). In diaphragm paralysis, the motion of the affected diaphragm was significantly lower compared to the contralateral normal diaphragm (-1.1 ± 2.2 mm vs. 7.6 ± 3.8 mm, $p = 0.005$). The normal diaphragms showed significantly greater motion than the paralyzed diaphragms (4.5 ± 2.1 mm vs. -1.1 ± 2.2 mm, $p < 0.0001$). On the contrary, the respiratory excursions of the normal diaphragms were significantly smaller than those of the contralateral normal diaphragms in diaphragm paralysis (4.5 ± 2.1 mm vs. 7.6 ± 3.8 mm, $p = 0.01$).

Basal Lung Density Change on 4D CT

The basal lung density changes between peak inspiration and expiration measured by 4D CT in various conditions are described in Table 2. In the 8 patients with normal diaphragms, there were no significant differences between the right and left basal lungs (134 ± 56 HU vs. 138 ± 79 HU, $p = 0.6$). In diaphragm paralysis, basal lung density change of the affected side was significantly smaller than that of the contralateral side (89 ± 73 HU vs. 180 ± 71 HU, $p = 0.03$). No significant differences in basal lung density change were found between the normal and paralyzed diaphragms (136 ± 66 HU vs. 89 ± 73 HU, $p = 0.1$) or between the normal and the contralateral normal diaphragms in diaphragm paralysis (136 ± 66 HU vs. 180 ± 71 HU, $p = 0.1$).

DISCUSSION

This study demonstrated the technical feasibility of 4D CT for the functional evaluation of the diaphragm in infants and young children. In all the patients, both diaphragms were completely included in the 3.8-cm longitudinal coverage of the CT system used in this study. However, longer z-axis coverage is necessary to include both diaphragms in older children and adults. In addition, the whole 4D CT scan duration of 2 seconds was long enough to include more than one respiratory cycle in all the patients. Although the fixed scan duration was used in this study, the scan duration of 4D CT may be reduced when respiratory rates are higher than 30 breaths per minute. In this study, the 4D CT findings of the diaphragm showed a high concordance rate (90.9%) with the sonographic data.

As in M-mode sonography, the respiratory excursion of the diaphragm could be quantified with 4D CT in various conditions including normal, paralysis, and eventration in this study. Compared with the normal diaphragms, the measured respiratory excursions on 4D CT were significantly reduced in the paralyzed diaphragms, and substantially

Korean Journal of Radiology
KJR

increased in the contralateral normal diaphragms in diaphragm paralysis. In M-mode sonography, diaphragm motion is considered normal if the respiratory excursion is greater than 4 mm, and the difference of excursion between the hemidiaphragms is less than 50% (4). Notably, the respiratory excursions measured with 4D CT were below 4 mm in 50% (8/16) of the normal diaphragms. The discrepancy may be attributed to the difference in patient age between the two studies: e.g., median age, 3.5 months; age range 3 days–3 years in this study vs. mean age, 1 year and 10 months; age range 3 days–17 years in the previous sonographic study (4). In this regard, the criteria of normal diaphragm motion needs to be stratified depending on patient size. Furthermore, it is noteworthy that this study clearly showed the augmented respiratory excursions of the contralateral normal diaphragms in diaphragm paralysis quantified with 4D CT, which has not been described in previous studies using M-mode sonography (4, 6).

One of the diagnostic pitfalls of M-mode sonography is that the magnitude of the measured diaphragm motion is subject to underestimation if the M-mode tracing is not orthogonal to diaphragm motion (4). On the contrary, the measurement of diaphragm motion with 4D CT is surely orthogonal to diaphragm motion because the measurement is fundamentally retrospective rather than prospective and it has no angle problem associated with M-mode tracing. In fact, such retrospective measurements with M-mode sonography are difficult and the M-mode tracing in this study, therefore, could not be retrospectively measured. In this study, 4D CT appeared to detect paradoxical motion of the paralyzed diaphragms more frequently (60.0% vs. 16.7%) than chest sonography. However, further study is required, with control of potential confounding factors and minimal inter-study intervals between 4D CT and chest sonography to validate the findings.

To determine the direction of motion of each hemidiaphragm correctly, it is critical to recognize the correct phases of the respiratory cycle during M-mode sonography. For an inexperienced imager, it may be difficult to see sonographic images and patient's breathing condition simultaneously. Moreover, it is not always possible to recognize the correct respiratory phase of the M-mode tracing based solely on the peak shape. However, the correct respiratory phase can be easily appreciated on 4D CT because lung density change and chest wall motion are simultaneously visualized throughout the respiratory cycle. The capability of 4D CT to evaluate the lung density change seems to be advantageous over chest sonography because reduced diaphragm motion secondary to pulmonary air trapping can be distinguished from primary diaphragm paralysis. In fact, diaphragm motion appeared to be reduced secondary to diffuse pulmonary air trapping in 1 patient exhibiting decreased basal lung density changes (14 HU for the right basal lung and 41 HU for the left basal lung) that are considerably smaller than those in normal lungs. The basal lung density changes on 4D CT were 136 ± 66 HU in normal diaphragms, but were significantly smaller in the paralyzed diaphragms (89 ± 73 HU) than in the contralateral normal diaphragms (180 ± 71 HU) in diaphragm paralysis. These results are in line with a previous study using cine-CT in 30 free-breathing young children that reported the lung density change between inspiration and expiration of 111 ± 49 HU in normal lungs and of -19 ± 34 HU in abnormal lungs with air trapping (12). In addition, the result of this study suggested that lung density changes in both basal lungs were influenced by the different amplitudes of the respiratory excursions of both hemidiaphragms in diaphragm paralysis.

Despite the great potential of 4D CT for the functional evaluation of the pediatric diaphragm demonstrated in this study, we should notice that 4D CT has an important limitation as a bedside imaging procedure. A majority of children who need functional diaphragm evaluations are managed in an intensive care unit and commonly mechanically ventilated. A bedside imaging procedure, therefore, is mandatory. As a mobile CT may offer a solution to the problem, such a mobile CT unit is not widely available. Moreover, the imaging capabilities, including 4D CT, may not match the quality of the state-of-the art-CT scanners. Hence, it is suggested that 4D CT should play a supplementary role for the functional evaluation of the pediatric diaphragm in selected patients with an appropriate clinical setting, and chest sonography remains as the primary imaging modality.

This study is limited by the small study population and retrospective nature. Consequently, the results were not sufficient to show the clinical usefulness of 4D CT of the diaphragm in comparison with a current reference imaging method, such as sonography. Therefore, a large-scale prospective comparative study is necessary to prove the diagnostic potential of 4D CT of the diaphragm. It appears to be a prerequisite that a mobile CT capable of 4D CT evaluation should be available in an intensive care unit in the future because most patients with severe diaphragmatic

abnormalities cannot leave an intensive care unit. Due to the retrospective nature of this study, there might be a selection bias in performing 4D CT, and only patients with milder clinical symptoms who could be moved to the CT room were actually included. Nevertheless, the potential supplementary role of 4D CT for the functional evaluation of the diaphragm could be demonstrated in this study in select patients. In fact, only a few representative cases using 4D CT for functional diaphragm evaluation have been recently reported, even in adult patients (13). Secondly, patient conditions might be different between 4D CT and sonography, due to inter-study interval, different respiratory difficulty, and being sedated or awake. The different patient conditions might affect the results of the comparison between the two imaging methods. Lastly, albeit a low radiation dose of 4D CT, it may have small risks associated with ionizing radiation that need to be reduced as much as possible. A study (14) reported that radiation dose of 4D CT may be additionally reduced by using a 4D CT penalized weighted least square smoothing method with reduced image noise and preserved spatial resolution.

In conclusion, the functional evaluation of the pediatric diaphragm is feasible with 4D CT in select children.

Supplementary Movie Legends

Movie 1. Normal diaphragm.
Movie 2. Diaphragm paralysis.

REFERENCES

1. Nason LK, Walker CM, McNeeley MF, Burivong W, Fligner CL, Godwin JD. Imaging of the diaphragm: Anatomy and function. *Radiographics* 2012;32:E51-E70
2. Kharma N. Dysfunction of the diaphragm: imaging as a diagnostic tool. *Curr Opin Pulm Med* 2013;19:394-398
3. Chavhan GB, Babyn PS, Cohen RA, Langer JC. Multimodality imaging of the pediatric diaphragm: anatomy and pathologic conditions. *Radiographics* 2010;30:1797-1817
4. Epelman M, Navarro OM, Daneman A, Miller SF. M-mode sonography of diaphragmatic motion: description of technique and experience in 278 pediatric patients. *Pediatr Radiol* 2005;35:661-667
5. Goo HW. Advanced functional thoracic imaging in children: from basic concepts to clinical applications. *Pediatr Radiol* 2013;43:262-268
6. Ayoub J, Cohendy R, Dauzat M, Targhetta R, De la Coussaye JE, Bourgeois JM, et al. Non-invasive quantification of diaphragm kinetics using m-mode sonography. *Can J Anaesth* 1997;44:739-744
7. Greenberg SB. Dynamic pulmonary CT of children. *Am J Roentgenol* 2012;199:435-440
8. Goo HW. Current trends in cardiac CT in children. *Acta Radiol* 2013;54:1055-1062
9. Tan JZ, Crossett M, Ditchfield M. Dynamic volumetric computed tomographic assessment of the young paediatric airway: Initial experience of rapid, non-invasive, four-dimensional technique. *J Med Imaging Radiat Oncol* 2013;57:141-148
10. Greenberg SB, Dyamenahalli U. Dynamic pulmonary computed tomography angiography: a new standard for evaluation of combined airway and vascular abnormalities in infants. *Int J Cardiovasc Imaging* 2014;30:407-414
11. Goo HW. Individualized volume CT dose index determined by cross-sectional area and mean density of the body to achieve uniform image noise of contrast-enhanced pediatric chest CT obtained at variable kV levels and with combined tube current modulation. *Pediatr Radiol* 2011;41:839-847
12. Goo HW, Kim HJ. Detection of air trapping on inspiratory and expiratory phase images obtained by 0.3-second cine CT in the lungs of free-breathing young children. *Am J Roentgenol* 2006;187:1019-1023
13. Wielpütz MO, Eberhardt R, Puderbach M, Weinheimer O, Kauczor HU, Heussel CP. Simultaneous assessment of airway instability and respiratory dynamics with low-dose 4D-CT in chronic obstructive pulmonary disease: a technical note. *Respiration* 2014;87:294-300
14. Li T, Schreibmann E, Thorndyke B, Tillman G, Boyer A, Koong A, et al. Radiation dose reduction in four-dimensional computed tomography. *Med Phys* 2005;32:3650-3660